

Offsite Autotuning Approach

Performance Model Driven Autotuning Applied to Parallel Explicit ODE Methods

Johannes Seiferth, Matthias Korch, Thomas Rauber

Department of Computer Science, University of Bayreuth, Bayreuth, Germany
{johannes.seiferth, korch, rauber}@uni-bayreuth.de

Abstract. Autotuning (AT) is a promising concept to minimize the often tedious manual effort of optimizing scientific application for a specific target platform. Ideally, an AT approach can reliably identify the most efficient implementation variant(s) for a new platform or new characteristics of the input by applying suitable program transformations and analytic models. In this work, we introduce Offsite, an offline AT approach which automates this selection process at installation time by rating implementation variants based on an analytic performance model without requiring time-consuming runtime tests. From abstract multilevel YAML description languages, Offsite automatically derives optimized, platform-specific and problem-specific code of possible variants and applies the performance model to these variants.

We apply Offsite to parallel numerical methods for ordinary differential equations (ODEs). In particular, we investigate tuning a specific class of explicit ODE solvers (PIRK methods) for four different initial value problems (IVPs) on three different shared-memory systems. Our experiments demonstrate that Offsite can reliably identify the set of most efficient implementation variants for different given test configurations (ODE solver, IVP, platform) and effectively handle important AT scenarios.

Keywords: Autotuning · performance modeling · description language
· ODE methods · ECM performance model · shared-memory

1 Introduction

The performance of scientific applications strongly depends on the characteristics of the targeted computing platform, such as, e.g., the processor design, the core topology, the cache architectures, the memory latency or the memory bandwidth. Facing the growing diversity and complexity of today's computing landscape, the task of writing and maintaining highly efficient application code is getting more and more cumbersome for software developers. A highly optimized implementation variant on one target platform, might, however, perform poorly on another platform. That particular poorly performant implementation variant, though, could again potentially outperform all other variants on the next platform. Hence, in order to achieve a high efficiency and obtain optimal performance when migrating an existing scientific application, developers need to tune and adapt the application code for each specific platform anew.

1.1 State of the Art

A promising concept to avoid this time-consuming, manual effort is **autotuning** (AT), and many different approaches have been proposed to automatically tune software [2]. AT is based on two core concepts: (i) the generation of optimized implementation variants based on program transformation and optimization techniques such as, e.g., loop unrolling or loop tiling, and (ii) the selection of the most efficient variant(s) on the target platform from the set of generated variants. In general, there are (i) **offline** and (ii) **online** AT techniques. Offline AT tries to select the supposedly most efficient variant at compile or installation time without actual knowledge of the input data. These approaches are applicable for use-cases, whose execution behavior does not depend on the input data. This is the case, e.g., for dense linear algebra problems, which can, i.a., be tuned offline with *ATLAS* [20] and *PhiPAC* [4]. In other fields, such as sparse linear algebra or particle codes, characteristics of the input data heavily influence the execution behavior. By choosing the best variant at runtime—when all input is known—, online AT approaches such as *Active Harmony* [19] and *ATF* [13] incorporate these influences.

Selecting a suitable implementation variant from a potentially large set of available variants in a time-efficient manner is a big challenge in AT. Various techniques and search strategies have been proposed in previous works to meet this challenge [2]. A straightforward approach is the time-consuming comparison of variants by runtime tests, possibly steered by a single search strategy, such as an exhaustive search or more sophisticated mathematical optimization methods like *differential evolution* [6], or a combination of multiple search strategies [1]. [12] proposes a hierarchical approach that allows the use of individual search algorithms for dependent subspaces of the search space. As an alternative to runtime tests, analytic performance models can be applied to either select the most efficient variant or to reduce the number of tests required by filtering out inefficient variants beforehand. In general, two categories of performance models are distinguished: (i) **black box models** applying statistical methods and machine learning techniques to observed performance data like hardware metrics or measured runtimes in order to learn to predict performance behavior [16,18], and (ii) **white box models** such as the *Roofline model* [21] or the *ECM performance model* [9,17] that describe the interaction of hardware and code using simplified machine models. For loop kernels, the *Roofline* and the *ECM model* can be automatically constructed with the *Kerncraft* tool [8].

1.2 Main Contributions

In this work, we propose **Offsite**, an offline AT approach that automatically identifies the most efficient implementation variant(s) during installation time based on performance predictions. These predictions stem from an analytic performance prediction methodology for explicit ODE methods proposed by [15] that uses a combined white and black box model approach based on the ECM model. The main contributions of this paper are:

```

1  for  $l \leftarrow 1, \dots, s$  do  $\mathbf{Y}_l^{(0)} \leftarrow \mathbf{y}_\kappa$ 
2  for  $k \leftarrow 1, \dots, m$  do
3    for  $l \leftarrow 1, \dots, s$  do
4       $\mathbf{Y}_l^{(k)} \leftarrow \mathbf{y}_\kappa + h_\kappa \sum_{i=1}^s a_{li} \mathbf{F}_i^{(k-1)}$  with  $\mathbf{F}_i^{(k-1)} \leftarrow \mathbf{f}(t_\kappa + c_i h_\kappa, \mathbf{Y}_i^{(k-1)})$ 
5   $\mathbf{y}_{\kappa+1} \leftarrow \mathbf{y}_\kappa + h_\kappa \sum_{i=1}^s b_i \mathbf{F}_i^{(m)}$ 
    
```

Listing 1. Timestep function of a PIRK method.

(i) We develop a novel offline AT approach for shared-memory systems based on performance modelling. This approach automates the task of generating the pool of possible implementation variants using abstract description languages. For all these variants, our approach can automatically predict their performance and identify the best variant(s). Further, we integrated a database interface for collected performance data which enables the reusability of data and which allows to include feedback from possible online AT or actual program runs.

(ii) We show how to apply Offsite to an algorithm from numerical analysis with complex runtime behavior: the parallel solution of IVPs of ODEs.

(iii) We validate the accuracy and efficiency of Offsite for different test configurations and discuss its applicability to four different AT scenarios.

1.3 Outline

Section 2 details the selected example use-case (PIRK methods) and the corresponding testbed. Based on this use-case, Offsite is described in Section 3. In Section 4, we experimentally evaluate Offsite in four different AT scenarios and on three different target platforms. Section 5 concludes the paper.

2 Use-Case and Experimental Test Bed

Use-Case: PIRK Methods

As example use-case, we investigate **parallel iterated Runge-Kutta** (PIRK). PIRK methods are part of the general class of explicit ODE methods [10] and solve an ODE System

$$\mathbf{y}'(t) = \mathbf{f}(t, \mathbf{y}(t)) \quad , \quad \mathbf{y}(t_0) = \mathbf{y}_0 \quad , \quad \mathbf{y} \in \mathbb{R}^n \quad (1)$$

by performing a series of timesteps until the end of the integration interval is reached. In each timestep, a new numerical approximation $\mathbf{y}_{\kappa+1}$ for the unknown solution \mathbf{y} is determined by an explicit predictor–corrector process in a fixed number of substeps.

PIRK methods are an excellent candidate class for AT. Their complex four-dimensional loop structure (Lst. 1) can be modified by loop transformations resulting in a large pool of possible implementation variants whose performance behavior potentially varies highly depending on: (i) the composition of computations and memory accesses, (ii) the number of stages of the base ODE method, (iii) the characteristics of the ODE system solved, (iv) the target hardware, (v) the compiler and the compiler flags, and (vi) the number of threads started.

Table 1. Characteristics of the test set of IVPs.

| IVP | Cusp | IC | Medakzo | Wave1D |
|-------------------------------------|-----------|---------------|-----------|--------------|
| Access distance ¹ | unlimited | limited | unlimited | limited |
| Computational behavior | mixed | compute-bound | mixed | memory-bound |

¹ In practice, many IVPs are sparse, i.e. only access few components of \mathbf{Y} when evaluating function \mathbf{f} (line 4, Lst. 1). A special case of sparse is *limited access distance* $d(\mathbf{f})$, where f_j only accesses components $y_{j-d(\mathbf{f})}$ to $y_{j+d(\mathbf{f})}$.

Table 2. Characteristics of the test set of target platforms.

| Name | HSW | IVB | SKY |
|--|-----------------|-----------------|----------------|
| Micro-architecture | Haswell EP | Ivy-Bridge EP | Skylake SP |
| CPU | Xeon E5-2630 v3 | Xeon E5-2660 v2 | Xeon Gold 6148 |
| Clock speed | 2.3 GHz | 2.2 GHz | 1.76 GHz |
| Cores | 8 | 10 | 20 |
| L1 cache (data) | 32 kB | 32 kB | 32 kB |
| L2 cache | 256 kB | 256 kB | 1 MB |
| L3 cache (shared) | 20 MB | 25 MB | 27.5 MB |
| Cache line size | 64 B | 64 B | 64 B |
| Instruction throughput per cycle (double precision) | | | |
| ADD / FMA / MUL | 2 / 1 / 1 | 1 / - / 1 | 4 / 2 / 4 |
| Compiler | icc 19.0.5 | icc 19.0.4 | icc 19.0.2 |

Test Set of Initial Value Problems

In our experiments, we consider a broad set of IVPs (Table 1) that exhibit different characteristics: *(i)* *Cusp* combines Zeeman’s cusp catastrophe model for a threshold-nerve-impulse mechanism with the van der Pol oscillator [7], *(ii)* *IC* describes a traversing signal through a chain of N concatenated inverters [3], *(iii)* *Medakzo* describes the penetration of radio-labeled antibodies into a tissue infected by a tumor [11], and *(iv)* *Wave1D* describes the propagation of disturbances at a fixed speed in one direction [5].

Test Set of Target Platforms

We conducted our experiments on three different shared-memory systems (Table 2). For all experiments, the CPU clock was fixed, hyper-threading disabled and thread binding set with `KMP_AFFINITY=granularity=fine,compact`. All codes were compiled with the Intel C compiler and compiler flags `-O3`, `-xAVX` and `-fno-alias` set.

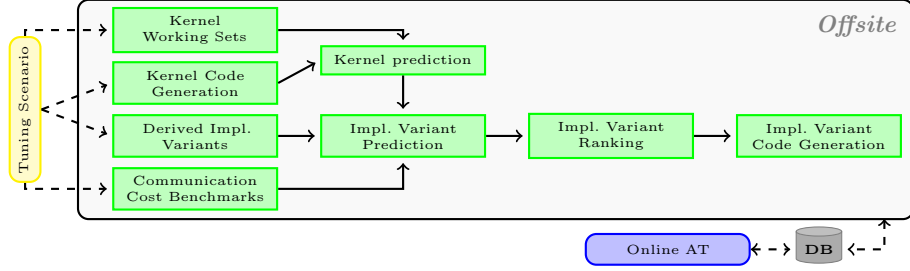


Fig. 1. Workflow of the Offsite autotuning approach.

3 Offsite Autotuning Approach

In this work, we introduce the **Offsite** offline AT approach on the example of explicit ODE methods. Before starting a new Offsite run, the *tuning scenario* desired, which consists of: (i) the pool of possible implementations and program transformations, (ii) the ODE base method(s), (iii) the IVP(s), and (iv) the target platform, is defined using description languages in the YAML standard¹.

From its input data, Offsite automatically handles the whole tuning workflow (Fig. 1). First, Offsite generates optimized, platform-specific and problem-specific code for all kernels and derives all possible implementation variants. Applying an analytic performance prediction methodology, the performance of each kernel is predicted for either (i) a fixed ODE system size n —if specified by the user or prescribed by the ODE²—or (ii) a set of relevant ODE system sizes determined by a working set model. The performance of a variant is derived by combining the predictions of its kernels and adding an estimate of its synchronization costs. Variants are ranked by their performance to identify the most efficient variant(s). All obtained prediction and ranking data are stored in a database. For the best ranked variants, Offsite generates optimized, platform-specific and problem-specific code.

3.1 Input Description Languages

A decisive, yet cumbersome step in AT is generating optimized code. Often, there is a large pool of possible implementation variants, applicable program transformations (e.g. loop transformations) and tunable parameters (e.g. tile sizes) available. Furthermore, exploiting characteristics of the input data can enable more optimizations (e.g. constant propagation). Writing all variants by hand, however, would be tedious and error-prone and there is demand for automation. In this work, we introduce multilevel description languages to describe implementations, ODE methods, IVPs and target platforms in an abstract way. Offsite can interpret these languages and automatically derives optimized code.

¹ YAML is a data serialization language; <https://yaml.org>

² There are scalable ODE systems but also ODEs with a fixed size [7].

```

1 stages: 4
2 order: 7
3 corrector_steps: 6
4 A: [[["0.1130", "-0.0403", "0.0258",
        "-0.0099"], ..., [...]]
5 b: ["0.2205", ...]
6 c: ["0.1130 - 0.0403 + 0.0258 -
        0.0099", ...]

```

Listing 2. ODE method description format on the example of *Radau IIA(7)*.

```

1 components:
2   first: 1
3   size: n-1
4   code: |
5     (((U_op - %in[j]) * R - (eta * ((%in[j]
        -1] - U_thres) * (%in[j-1] -
        U_thres) - (%in[j-1] - %in[j] -
        U_thres) * (%in[j-1] - %in[j] -
        U_thres)))) / C);
6 constants:
7   - double R = 1.0
8   - ...

```

Listing 3. IVP description format on the example of *InverterChain*.

The Base ODE Method of a PIRK method is characterized by its Butcher table—i.e., coefficient matrix A , weight vector b , node vector c —and a small set of properties: (i) number of stages s , (ii) order o , (iii) number of corrector steps m . Exploiting these properties, however, can have a large impact on the efficiency of an implementation variant and should be included into the code generation in order to obtain the most efficient code. The i -loop in Listing 4, e.g., might be replaceable by a single vector operation for specific s , or zero entries in the Butcher table might allow to save computations.

Listing 2 shows the ODE method description format on the example of *Radau IIA(7)* which is a four-stage method with order seven applying six corrector steps per timestep. To save space, only an excerpt of the Butcher table is shown with a reduced number of digits.

IVPs are described in the IVP description format shown by *IC* (Lst. 3):

(i) components describes the n components of the IVP. Each component contains a code YAML block that describes how function evaluation $\mathbf{f}(t_\kappa + c_i h_\kappa, \mathbf{Y}_i^{(k-1)})$ (l. 4, Lst. 1) will be substituted during code generation whereby %in is a placeholder for the used input vector $\mathbf{Y}_i^{(k-1)}$. Adjacent components that execute the same computation can be described by a single block whereby first denotes the first component and size specifies the total number of adjacent components handled by that particular block.

(ii) constants defines IVP-specific parameters replaced with their actual values during code generation and might possibly enable further code optimizations. In IVP *IC*, e.g., a multiplication could be saved if the given electrical resistance R equals 1.0.

Target Platform and Compiler are described using the machine description format introduced by Kerncraft³. Its general structure is tripartite: (i) the execution architecture description, (ii) the cache and memory hierarchy description, and (iii) benchmark results of typical streaming kernels.

³ For example files, we refer to <https://github.com/RRZE-HPC/kerncraft>.

```

1 datastructs:
2   - double b[s]
3   - double F[s][n]
4   - double dy[n]
5 computations:
6   C1: "dy[j] = dy[j] + b[i] * F[i][j]"
7 variants:
8   - name: APRX_ij
9     code: |
10      %PRAGMA nounroll_and_jam
11      %LOOP_START i s
12      %LOOP_START j n
13      %COMP C1
14      %LOOP_END j
15      %LOOP_END i
16   working sets: { "(s+1)*n+s", "2*n" }
17   - name: APRX_ji
18     code: |
19      %LOOP_START j n
20      %LOOP_START i s unroll
21      %COMP FMA
22      %LOOP_END i
23      %LOOP_END j
24   working sets: { "(s+1)*n+s" }

```

Listing 4. Kernel template description YAML on the example of *APRX*.

```

1 double F[4][1912]; // s=4; n=161
2 double dy[1912]; // n=161
3 for (int j=0; j<161; ++j) { // n=161;
4   unrolled i; replaced b[i]
5   dy[0] += 0.2205 * F[0][j];
6   dy[1] += 0.3882 * F[1][j];
7   dy[2] += 0.3288 * F[2][j];
8   dy[3] += 0.0625 * F[3][j];
9 }

```

Listing 5. Code generated for kernel *APRX_ji* of kernel template *APRX* specialized on *Radau IIA(7)* & $n = 161$.

```

1 code: |
2   %COM omp_barrier
3   %LOOP_START k m
4   %KERNEL RHS
5   %COM omp_barrier
6   %KERNEL LC
7   %COM omp_barrier
8   %LOOP_END k
9   %KERNEL RHS
10  %COM omp_barrier
11  %KERNEL APRX
12  %KERNEL UPD

```

Listing 6. Implementation skeleton description format on the example of *A*.

```

1 void timestep(...) {
2   #omp barrier
3   for (k=0; k<6; ++k) { // m=6
4     // Code for kernel template RHS
5     #omp barrier
6     // Code for kernel template LC
7     #omp barrier
8   }
9   #omp barrier
10  // Code for kernel template RHS
11  // Kernel APRX
12  for (int j=0; j<161; ++j) { // n=161;
13    unrolled i; replaced b[i]
14    dy[0] += 0.2205 * F[0][j];
15    dy[1] += 0.3882 * F[1][j];
16    dy[2] += 0.3288 * F[2][j];
17    dy[3] += 0.0625 * F[3][j];
18  }
19  // Code for kernel template UPD
20 }

```

Listing 7. Code generated for a variant of impl. skeleton *A* using kernel *APRX_ji* specialized on *Radau IIA(7)* & $n = 161$.

Implementation Variants of numerical algorithms are abstracted by description languages as (i) **kernel templates** and (ii) **implementation skeletons**.

Kernel Templates define basic computation kernels and possible variations of this kernel enabled by program transformations that preserve semantic correctness. Listing 4 shows the kernel template description format on the example of *APRX*, which covers computation $\sum_{i=1}^s b_i \mathbf{F}_i^{(m)}$ (l. 5, Lst. 1):

(i) *datastructs* defines required data structures.

(ii) *computations* describes the computations covered by a kernel template. Each computation corresponds to a single line of code and has a unique identifier (E.g. *C1* in Lst. 4). Computations can contain IVP evaluations which are marked by keyword *%RHS* and are replaced by an IVP component during code generation (E.g. for *IC* by line 5 of Lst. 3). Hence, if a kernel template contains *%RHS*, a separate, specialized kernel version has to be generated for each IVP component.

(iii) variants contains possible kernels of a kernel template enabled by program transformations. For each kernel, its workings sets (working sets) and its program code (code) are specified. A code block defines for a kernel its order of computations and program transformations and using four keywords. Computations are specified by keyword %COMP whose parameter must correspond to one of the identifiers defined in the computations block (E.g. *C1* in Lst. 4). For-loop statements are defined by %LOOP_START and %LOOP_END. The first parameter of %LOOP_START specifies the loop variable name, the second the number of loop iterations and an optional third parameter unroll indicates that the loop will be unrolled during code generation. Loop-specific pragmas can be added using %PRAGMA.

Implementation skeletons define processing orders of kernel templates and required communication points. From skeletons, concrete implementation variants are derived by replacing its templates with concrete kernel code. Listing 6 shows the implementation skeleton description format on the example of skeleton *A* which is a realization of a PIRK method (Lst. 1) that focuses on parallelism across the ODE system, i.e its n equations are distributed blockwise among the threads. *A* contains a loop k over the m corrector steps dividing each corrector step into two templates: *RHS* computes the IVP function evaluations (l. 5, Lst. 1) which are used to compute the linear combinations (l. 4, Lst. 1) in *LC*. Per corrector step, two synchronizations are needed as *RHS*—depending on the IVP solved—can potentially require all components of the linear combinations from the last iteration of k . After all corrector steps are computed, the next approximation $\mathbf{y}_{\kappa+1}$ is calculated by templates *APRX* and *UPD* (l. 6, Lst. 1). Four keywords suffice to specify skeletons:

- (i) %LOOP_START and %LOOP_END define for-loops.
- (ii) %COM states communication operations of an implementation skeleton. Skeleton *A*, e.g., requires $2m + 2$ barrier synchronizations.
- (iii) %KERNEL specifies an executed kernel template. Its parameter must correspond to the name of a kernel template. During code generation %KERNEL is replaced by actual kernel code (e.g. *APRX* in Lst. 7).

3.2 Rating Implementation Variant Performance

Offsite can automatically identify the most efficient implementation variant(s) from a pool of available variants using analytic performance modelling (Fig. 1):

- (i) In a first step, Offsite automatically generates code for all kernels in a special code format processable by kerncraft⁴. Kernel code generation (*Kernel Code Generation* in Fig. 1) includes specializations of the code on the target platform, IVP, ODE method and (if fixed) ODE system size n . Listing 5 exemplary shows the code generated for kernel *APRX_{ji}* of kernel template *APRX* (Lst. 4) when specialized on ODE method *Radau IIA(7)* and $n = 161$. As specified in the template description, j loop is unrolled completely. Further, Butcher table coefficients (**b**) and known constants ($s = 4$, $n = 161$) are substituted.

⁴ In this work, version 0.8.3 of the Kerncraft tool was used.

(ii) In some tuning scenarios, the ODE system size n is not yet known during installation time. Giving predictions for all valid n values, however, is in general not feasible. By applying a working set model (Sec. 3.4), Offsite automatically determines for each kernel a set of relevant n (*Kernel Working Sets*, Fig. 1) for which predictions are then obtained in the next step.

(iii) Offsite automatically computes node-level runtime predictions (Sec. 3.3) for each implementation variant (*Impl. Variant Prediction*, Fig. 1) by adding up the kernel predictions of its kernels and adding an estimate of its communication costs (*Communication Cost Benchmarks*, Fig. 1), which Offsite derives from benchmark data. For each of the kernel codes generated in step (i), its kernel prediction is automatically derived by Offsite (*Kernel Prediction*, Fig. 1) whereby Kerncraft is used to construct the ECM model.

(iv) Using these node-level runtime predictions, Offsite ranks implementation variants by their performance (*Impl. Variant Ranking*, Fig. 1).

(v) From the ranking of implementation variants, Offsite automatically derives the subset Λ of the best rated variant(s) which contains all variants λ whose performance is within an user-provided maximum deviation from the best rated variant. For each variant of λ , Offsite generates optimized, platform-specific and problem-specific code (*Impl. Variant Code Generation*, Fig. 1). Listing 7 shows an excerpt of the code generated for an variant of implementation skeleton A which substitutes kernel template $APRX$ with kernel $APRX_ji$ and was specialized on ODE method *Radau IIA*(7), IVP *IC* and $n = 161$.

3.3 Performance Prediction Methodology

The performance prediction methodology applied by Offsite expands on the works of [15] and comprises: (i) a node-level runtime prediction of an implementation variant and (ii) an estimate of its intra-node communication costs.

Node-level Runtime Prediction. Base of the node-level prediction is the analytic *ECM (Execution-Cache-Memory) performance model*. For an in-depth explanation, we refer to [17,9]. The ECM model gives an estimation of the number of CPU cycles per cache line (CL) required to execute a particular loop kernel on a multi- or many-core chip which includes contributions from the in-core execution time T_{core} and the data transfer time T_{data} :

$$T_{\text{core}} = \max(T_{\text{OL}}, T_{\text{nOL}}) , \quad (2)$$

$$T_{\text{data}}^{\text{L3}} = T_{\text{L1L2}}^{\text{data}} + T_{\text{L2L3}}^{\text{data}} + T_{\text{L2L3}}^{\text{P}} . \quad (3)$$

T_{core} is defined as the time required to retire the instructions of a single loop iteration under the assumptions that (i) there are no loop-carried dependencies, (ii) all data are in the L1 data cache, (iii) all instructions are scheduled independently to the ports of the units, and (iv) the time to retire arithmetic instructions and load/store operations can overlap due to speculative execution depending on the target platform. Hence, the unit that takes the longest to retire

its instructions determines T_{core} . $T_{\text{data}}^{\text{level}}$ factors in the time required to transfer all data from its current location in the memory hierarchy to the L1 data cache and back. The single contributions of transfers between levels i and j of the memory hierarchy T_{ij}^{data} are determined depending on the amount of transferred CLs. Depending on the platform used, an optional latency penalty T_{ij}^p might be added. In (3) $T_{\text{data}}^{\text{level}}$ is exemplarily shown for data coming from the L3 cache under the assumption that a latency penalty between L2 and L3 cache has to be factored in on the platform used. Combining all contributions, a single-core prediction

$$T_{\text{ECM}}^{\text{level}} = \max(T_{\text{OL}}, T_{\text{nOL}} + T_{\text{data}}^{\text{level}}) \quad (4)$$

can be derived, whereby the overlapping capabilities of the target platform determine whether a contribution is considered overlapping or non-overlapping.

Using Kerncraft, Offsite obtains ECM model predictions (4) for all kernels λ . For each kernel, *kernel runtime prediction*

$$\phi_\lambda = \frac{\alpha_\lambda \cdot \beta_\lambda}{\delta \cdot f} \quad (5)$$

yields the runtime in seconds of kernel λ , where α_λ is (4) computed for a specific number of running cores τ , β_λ is the number of loop iterations executed, δ is the number of data elements fitting into one CL and f is the CPU frequency. By summing up the individual kernel runtime predictions ϕ_λ of its basic kernels λ and adding an estimate of its communication costs t_{com} , the *node-level runtime prediction* θ_ϵ of an implementation variant ϵ is given by:

$$\theta_\epsilon = \sum_{\lambda} \phi_\lambda + t_{\text{com}} \quad (6)$$

Remark: [15] used an older *Kerncraft* version that could not yet return ECM predictions for multiple core counts τ with a single run, but additionally returned the kernel’s saturation point σ_λ . Hence, an extra factor $\min(\tau, \sigma_\lambda)$ was needed in the denominator of (5) in their work.

Estimate of Intra-node Communication Costs. For the implementation variants considered in this work, the costs of the required OpenMP barrier operations are estimated depending on the number of threads using linear regression.

Reusability of Performance Predictions. Prediction data (e.g. kernel runtime predictions) collected for a specific implementation variant can be reused to estimate other variants (if they also include that kernel) or to estimate other IVPs (if the kernel does not contain any IVP evaluations). In the context of AT, this is a decisive advantage compared to time-consuming runtime testing of variants which requires running each additionally added variant as well or to run all variants anew when changing the IVP solved.

3.4 Working Set Model

If the ODE system size n is not fixed—either by the user or restrictions of the IVP—selecting the most efficient implementation variant(s) at installation time leads to an exhaustive search over the possibly vast space of values for n . To minimize the number of predictions required per kernel, the set of estimated n values is reduced by a model-based restriction, the **working set** of the kernel, which corresponds to the amount of data referenced by a kernel.

We use the working sets to identify for each kernel the maximum n that still fit into the single cache levels. Using these maximums, ranges of consecutive n values for which the ECM prediction (4) stays constant⁵ can be derived. The medium values of these ranges form the working set of the kernel.

4 Experimental Evaluation

We validate Offsite using the experimental test bed introduced in Section 2. In particular, we study the efficiency of Offsite in four AT scenarios when tuning four different IVPs on three different target platforms and compare the efficiency of the following AT strategies:

- (i) *BestVariant* covers the case that the most efficient implementation variant is already known (e.g. from previous execution) and no AT is required.
- (ii) *RunAll* runs all variants in order to identify the most efficient variant.
- (iii) *OffsitePreselect5* runs an Offsite determined subset of all variants, which contains all variants withing a 5 % deviation of the best ranked variant, to identify the most efficient variant of that subset.
- (iv) *OffsitePreselect10* runs variants within a 10 % deviation of the best variant.
- (v) *RandomSelect* randomly runs 20 of the total 56 variants.

4.1 Derived Implementation Variants

Table 3 summarizes the implementation skeletons and kernel templates used in this work. In total, we consider eight skeletons from which 56 implementation variants can be derived. Each table column shows the templates required by a particular skeleton. E.g., skeleton *A* (Lst. 6) uses templates *LC*, *RHS*, *APRX* and *UPD* and twelve variants can be derived from *A* as there are six different kernels of *LC* (enabled by loop interchanges, unrolls, pragmas) and two of *APRX*.

In total, 17 different kernels can be derived from the eight kernel templates available. To predict the performance of all 56 variants, only these 17 kernels have to be estimated. Further, when obtaining predictions off all 56 variants for a different IVP, only those four templates that contain IVP evaluations—and thus their six corresponding kernels—need to be re-evaluated, while prediction data of the remaining kernels can be retrieved from database.

⁵ The ECM prediction factors in the location of data in the memory hierarchy. As a simplified assumption—neglecting overlapping effects at cache borders—, this means that as long as data locations do not change, the ECM model yields the same value for a kernel independent from the actual n .

Table 3. Overview of the implementation variants considered.

| Impl. Skeleton (#Impl. Variants) | Kernel Template ¹ (#Kernels) | | | | | | | |
|-------------------------------------|---|---------|-----------|---------|-------------|--------|------------|----------------|
| | LC(6) | RHS*(1) | RHSLC*(1) | APRX(2) | RHSAPRX*(2) | UPD(1) | APRXUPD(2) | RHSAPRXUPD*(2) |
| A (12) | x | x | | x | | x | | |
| B (12) | x | x | | | | | x | |
| C (2) | | | x | x | | x | | |
| D (2) | | | x | | | | x | |
| E (2) | | | x | | x | x | | |
| F (2) | | | x | | | | | x |
| G (12) | x | x | | | x | x | | |
| H (12) | x | x | | | | | | x |

¹ A kernel template marked with * contains evaluations of the IVP.

4.2 AT Scenario – All Input Known

As first test scenario, we consider the case that all input is known at installation time, in particular the ODE system size n . In such cases, Offsite is applied without the working set model. Performance predictions, however, are only obtained for that particular n and a new Offsite AT run would be required if n changes.

Table 4 compares the accuracy and efficiency of AT strategies when tuning four different IVPs on three different target platforms for $n = 36,000,000$ and ODE method *Radau IIA*(7). For AT strategies *OffsitePreselect5* and *OffsitePreselect10*, t_{step} yields the time in seconds it takes to execute a timestep using the measured best implementation variant from the subset A of variants λ tested by that strategy. *Performance loss* denotes the percent runtime deviation of that particular measured best variant from the variant selected by *BestVariant* (t_{best}). Ideally, an AT strategy correctly identifies the measured best variant and, thus, would suffer no performance loss. For an AT strategy, $|A|$ yields the cardinality of subset A and the percent *tuning overhead* of applying that strategy is defined as $\frac{t_{\text{tune}} - |A|t_{\text{best}}}{|A|t_{\text{best}}} \cdot 100$ where $t_{\text{tune}} = \sum_{\lambda} t_{\lambda}$ is the time required to test all variants and $|A|t_{\text{best}}$ is the time needed to execute the measured best variant instead.

Haswell. AT strategy *RunAll* causes a significant tuning overhead for all IVPs, while *OffsitePreselect5* and *OffsitePreselect10* only lead to marginal overhead as the subset of tested variants is considerably smaller, while still being able to select the measured best variant for all IVPs but *Wave1D*.

IvyBridge. Again, *RunAll* leads to decisive overhead compared to both Offsite strategies and the measured best variant is correctly identified for all IVPs. However, for IVP *IC* only *OffsitePreselect10* finds the best variant. As *IC* is compute-bound (Table 1), the IVP evaluation dominates the computation time while the order of the remaining computations has only minor impact. Hence, already minor jitter can lead to a different variant being selected.

Skylake. Similar observations as on the two previous systems can be made. The overhead of both Offsite strategies is marginal compared to *RunAll*. For all IVPs, the measured best variant is successfully identified.

Table 4. Comparison of different AT strategies applied to four different IVPs with $n = 36,000,000$ and *Radau IIA*(7).

| | IVP | Cusp | IC | Medakzo | Wave1D |
|----------------------|---|----------|------------|----------|-------------|
| Haswell (8 cores) | BestVariant | F_*ji | F_*ij | F_*ji | H_LCjli_*ij |
| | BestVariant t_{step} [s] | 1.28 | 0.80 | 1.29 | 1.04 |
| | AT strategy – OffsitePreselect5 | | | | |
| | A (tuning overhead) | 3 (1%) | 3 (3%) | 2 (2%) | 3 (5%) |
| | t_{step} [s] selected variant (perf. loss) | 1.28 (–) | 0.80 (–) | 1.29 (–) | 1.08 (4%) |
| | AT strategy – OffsitePreselect10 | | | | |
| | A (tuning overhead) | 3 (1%) | 3 (3%) | 3 (1%) | 4 (5%) |
| | t_{step} [s] selected variant (perf. loss) | 1.28 (–) | 0.80 (–) | 1.29 (–) | 1.08 (4%) |
| | AT strategy – RunAll | | | | |
| | A (tuning overhead) | 56 (42%) | 56 (44%) | 56 (20%) | 56 (16%) |
| IvyBridge (10 cores) | BestVariant | E_*ji | F_*ij | F_*ji | F_*ji |
| | BestVariant t_{step} [s] | 1.16 | 0.725 | 1.20 | 1.04 |
| | AT strategy – OffsitePreselect5 | | | | |
| | A (tuning overhead) | 3 (3%) | 1 (1%) | 3 (1%) | 3 (0.4%) |
| | t_{step} [s] selected variant (perf. loss) | 1.16 (–) | 0.734 (1%) | 1.20 (–) | 1.04 (–) |
| | AT strategy – OffsitePreselect10 | | | | |
| | A (tuning overhead) | 3 (3%) | 3 (3%) | 3 (1%) | 3 (0.4%) |
| | t_{step} [s] selected variant (perf. loss) | 1.16 (–) | 0.725 (–) | 1.20 (–) | 1.04 (–) |
| | AT strategy – RunAll | | | | |
| | A (tuning overhead) | 56 (54%) | 56 (59%) | 56 (41%) | 56 (44%) |
| Skylake (20 cores) | BestVariant | E_*ji | F_*ji | F_*ji | F_*ji |
| | BestVariant t_{step} [s] | 0.43 | 0.24 | 0.45 | 0.40 |
| | AT strategy – OffsitePreselect5 | | | | |
| | A (tuning overhead) | 3 (1%) | 3 (2%) | 3 (1%) | 3 (%) |
| | t_{step} [s] selected variant (perf. loss) | 0.43 (–) | 0.24 (–) | 0.45 (–) | 0.40 (–) |
| | AT strategy – OffsitePreselect10 | | | | |
| | A (tuning overhead) | 3 (1%) | 3 (2%) | 3 (1%) | 3 (1%) |
| | t_{step} [s] selected variant (perf. loss) | 0.43 (–) | 0.24 (–) | 0.45 (–) | 0.40 (–) |
| | AT strategy – RunAll | | | | |
| | A (tuning overhead) | 56 (69%) | 56 (65%) | 56 (41%) | 56 (44%) |

4.3 AT Scenario – Unknown ODE System Size

The next scenario considered is that of a still unknown ODE system size n at installation time. In these cases, the working set model is applied to determine a set of sample n values for which Offsite computes predictions and from which predictions for the whole range of possible n are derived. As this requires computing multiple performance predictions, a single Offsite run takes longer than in the previous scenario. This particular Offsite run, however, already covers all possible n and no further run will be required when switching n at a later point.

Figures 2 and 3 show for the single implementation variants selected as best variant by the AT strategies considered, the time per timestep of *IC* and *Cusp* on three platforms (each using their max. number of cores). On the x-axis, n is

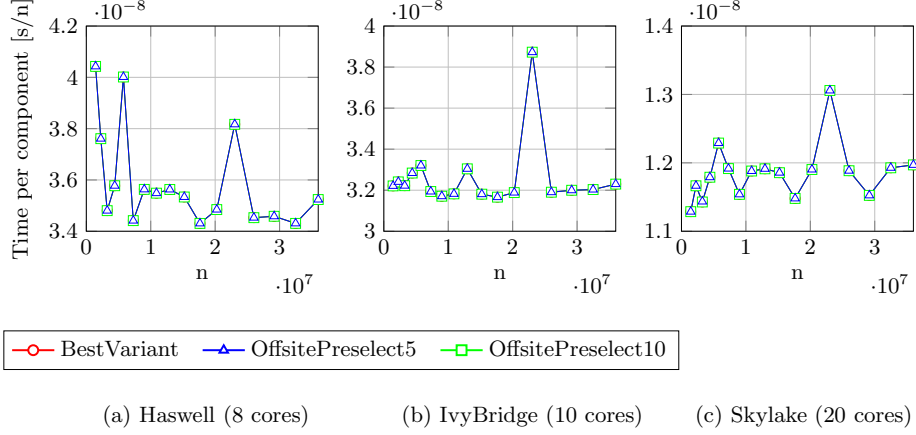


Fig. 2. Comparison of AT strategies applied to *Cusp* with varying n and *Radau IIA*(7).

plotted up to $n = 60,000,000$. The y-axis shows the time per component of n in seconds needed by a specific variant to solve a timestep for *Radau IIA*(7).

Tuning Cusp (Fig. 2). On *Haswell* (Fig. 2a), *OffsitePreselect5* and *OffsitePreselect10* select the same subset of three variants independent of n . Both strategies always correctly identify the measured best variant. The same observations can be made on *IvyBridge* (Fig. 2b) and on *Skylake* (Fig. 2c) where also the same subset of three variants is selected and the measured best variant is always found.

Tuning IC (Fig. 3). On *Haswell* (Fig. 3a), the same subset of one (for *OffsitePreselect5*) respectively of two variants (for *OffsitePreselect10*) is picked for n up to 8,500,000. For bigger n , both strategies select the same three variants. Except for $n = 5,760,000$, *OffsitePreselect10* always correctly finds the measured best variant. The single variant selected by *OffsitePreselect5* is slightly off for $n = 1,440,000$ and $n = 2,560,000$. In both cases, however, the absolute time difference is only marginal. *IC* is compute-bound (Table 1) and, thus, the IVP evaluation dominates the computation time. Hence, in particular for small n , the order of the remaining computations has only minor impact on the time and already minor jitter can lead to a different variant being selected.

OffsitePreselect5 selects on *IvyBridge* (Fig. 3b) the same variant for all n while *OffsitePreselect10* adds two additional variants for $n \geq 2,560,000$. While *OffsitePreselect10* always finds the measured best variant, *OffsitePreselect5* is slightly off for $n = 4,000,000$ and $n = 5,760,000$ but the absolute time difference is only marginal.

On *Skylake* (Fig. 3c), the same variant is selected for n up to 1,440,000 by *OffsitePreselect5* as well as by *OffsitePreselect10* while for larger n two additional

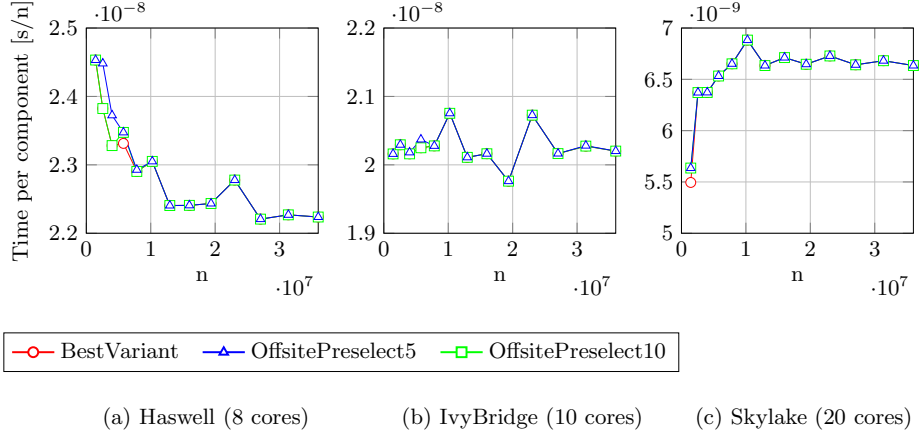


Fig. 3. Comparison of AT strategies applied to *IC* with varying n and *Radau IIA*(7).

variants are considered. Except for $n = 1,440,000$ both Offsite strategies manage to always correctly identify the measured best variant. As on the two previous systems, the absolute time difference is again only marginal.

4.4 AT Scenario – Variable Number of Cores

Offsite is capable of predicting the performance of an implementation variant for different core counts with a single AT run. In this AT scenario, we consider tuning an IVP for a fixed ODE system size n and multiple core counts.

Figure 4 shows the effectiveness of different AT strategies compared to strategy *RunAll* when tuning IVP *IC* on three target platforms for $n = 9,000,000$ and *Radau IIA*(7). On the x -axis, we plot the number of cores. The y -axis plots for different AT strategies the percent *performance gain* Π achieved by applying that particular strategy instead of *RunAll* which tests all 56 variants (t_{RA}). The performance gain is defined as $\frac{t_{RA} - t_{AT}}{t_{RA}} * 100$ where t_{AT} includes the time to run the variants A tested by that strategy and the time to run the measured best variant from A an additional $56 - |A|$ times. Ideally, the bar of an AT strategy would be close to the horizontal line of *BestVariant*.

Haswell (Fig. 4a). Depending on the number of cores, *OffsitePreselect5* picks different subsets A . For core counts smaller than eight, the same variant is selected, while for eight cores two additional variants are selected. Using *OffsitePreselect10*, these two variants are also included for four cores. For all core counts, a significant performance gain close to *BestImplVariant* can be observed when using the Offsite strategies. The total performance gain grows with increasing number of cores as the performance gap between best and worst variants also increases. While outperforming *RunAll*, *RandomSelect* is still far off from the maximum gain.

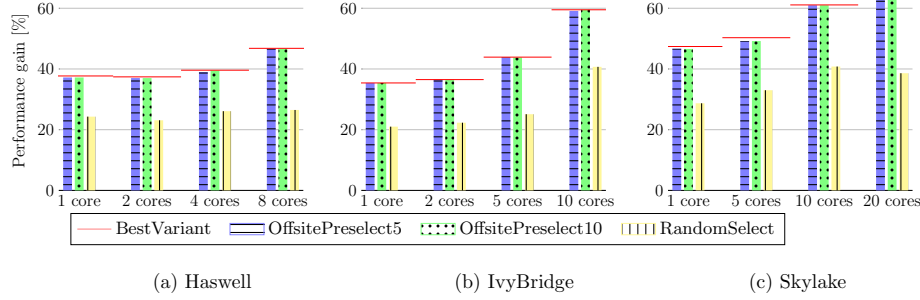


Fig. 4. Percent performance gain achieved by different AT strategies when tuning IVP IC for different core counts, *Radau IIA(7)* and $n = 9,000,000$.

IvyBridge (Fig. 4b). *OffsitePreselect5* selects the same variant for all core counts. Using *OffsitePreselect10*, only for 20 cores two further variants are selected. Again, a significant performance gain close to *BestImplVariant*, can be observed for all core counts when using the Offsite strategies while *RandomSelect* is far off from that ideal gain.

Skylake (Fig. 4c). Both Offsite strategies select the same three variants for 20 cores, while the same single variant is selected for smaller core counts. As on the two previous target platforms, both Offsite strategies are close too *BestImplVariant* while *RandomSelect* is again further off.

4.5 AT Scenario – Variable ODE Method

In the last AT scenario, we consider tuning an IVP for a fixed ODE system size n for four different ODE methods. Depending on the characteristics of the ODE method, different optimizations might be applicable—for specific number of stages s , e.g., loops over s can be replaced by a vector operation—which potentially results in varying efficiency of the same implementation variant for different ODE methods.

Figure 5 shows the effectiveness of different AT strategies when tuning IVP IC on three target platforms for $n = 9,000,000$ and four different ODE methods: (i) *Radau IA(5)* ($s = 3, m = 4$), (ii) *Radau IIA(7)* ($s = 4, m = 6$), (iii) *Lobatto IIIC(6)* ($s = 4, m = 5$), and (iv) *Lobatto IIIC(8)* ($s = 5, m = 7$). On the x -axis the ODE method used is shown. The y -axis plots for each AT strategy the percent performance gain Π achieved by applying that particular strategy instead of *RunAll* which tests all 56 variants. The bar of an AT strategy is ideally close to the horizontal line of *BestVariant*.

Tuning Haswell (Fig. 5a). *OffsitePreselect5* selects the same subset of two variants for *Lobatto IIIC(6)* and *Radau IA(5)*. For *Lobatto IIIC(8)* and *Radau IIA(7)*, an additional variant is selected. Using *OffsitePreselect10*, these three

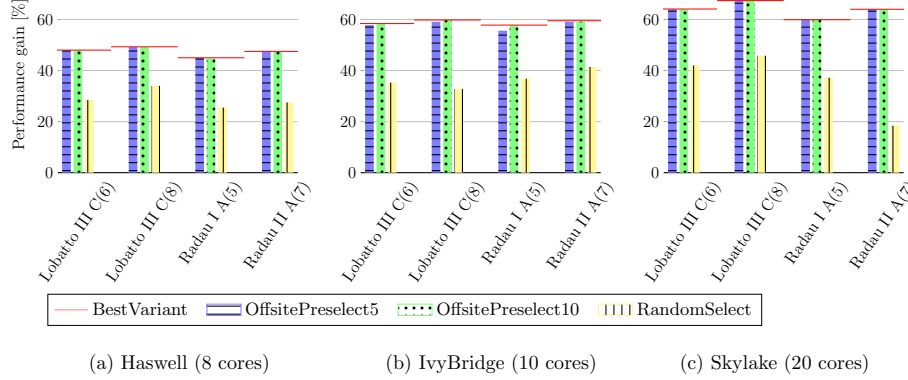


Fig. 5. Percent performance gain achieved by different AT strategies when tuning IVP IC for different ODE methods and $n = 9,000,000$.

variants are selected for all ODE methods. For all ODE methods, a significant performance gain close to *BestImplVariant* can be observed when using one of the two Offsite strategies. Further, both Offsite strategies decisively outperform *RandomSelect*.

IvyBridge (Fig. 5b). For all ODE methods, the same single variant is chosen when using *OffsitePreselect5*, while *OffsitePreselect10* selects two variants for *Lobatto III C(6)* and the same three variants for *Lobatto III C(8)* and *Radau II A(7)*. As on *Haswell*, the performance gain of both Offsite strategies for all ODE methods is close to the maximum gain, while the achieved gain of *RandomSelect* is far off from *BestImplVariant*.

Skylake (Fig. 5c). Both Offsite AT strategies select the same subset of three variants for all ODE methods but for *Radau I A(5)* which only selects two variants when using *OffsitePreselect5*. Again, the performance gain achieved by both Offsite strategies is close to *BestVariant* while *RandomSearch* is further off.

5 Conclusion and Future Work

In this work, we have introduced the Offsite AT approach which automates the process of identifying the most efficient implementation variant(s) from a pool of possible variants at installation time. Offsite ranks variants by their performance using analytic performance predictions. To facilitate specifying tuning scenarios, multilevel YAML description languages allow to describe these scenarios in an abstract way and enable Offsite to automatically generate optimized codes. Moreover, we have demonstrated that Offsite can reliably tune a representative class of parallel explicit ODE methods, PIRK methods, by investigating different AT scenarios and AT strategies on three different shared-memory platforms.

Our future work includes expanding Offsite to cluster systems as well as to AMD and ARM platforms. Further, we intend to extend Offsite to a combined offline-online AT approach that incorporates feedback data from previous online AT (or program runs) and to study whether these data can be used to predict the performance in scenarios with unknown input data (e.g. new IVP).

Acknowledgments

This work is supported by the German Ministry of Science and Education (BMBF) under project number 01IH16012A. Furthermore, we thank the Erlangen Regional Computing Center (RRZE) for granting access to their IvyBridge and Skylake systems.

References

1. Ansel, J., Kamil, S., Veeramachaneni, K., Ragan-Kelley, J., Bosboom, J., O'Reilly, U.M., Amarasinghe, S.: OpenTuner: An Extensible Framework for Program Autotuning. In: Proc. 23rd Int. Conf. on Parallel Architecture and Compilation Techniques. pp. 303–316. PACT '14, ACM (Aug 2014). <https://doi.org/10.1145/2628071.2628092>
2. Balaprakash, P., Dongarra, J., Gamblin, T., Hall, M., Hollingsworth, J.K., Norris, B., Vuduc, R.: Autotuning in High-Performance Computing Applications. Proceedings of the IEEE **106**(11), 2068–2083 (Nov 2018). <https://doi.org/10.1109/JPROC.2018.2841200>
3. Barthel, A., Günther, M., Pulch, R., Rentrop, P.: Numerical Techniques for Different Time Scales in Electric Circuit Simulation. In: High Performance Scientific and Engineering Computing: Proc. 3rd Int. FORTWIHR Conf. HPSEC. pp. 343–360. HPSEC' 02, Springer (Mar 2002). https://doi.org/10.1007/978-3-642-55919-8_38
4. Bilmes, J., Asanovic, K., Chin, C.W., Demmel, J.: Optimizing Matrix Multiply Using PHiPAC: A Portable, High-performance, ANSI C Coding Methodology. In: Proc. 11th Int. Conf. on Supercomputing. pp. 340–347. ICS '97, ACM (Jul 1997). <https://doi.org/10.1145/263580.263662>
5. Calvo, M., Franco, J.M., Ranz, L.: A New Minimum Storage Runge-Kutta Scheme for Computational Acoustics. Journal of Computational Physics **201**(1), 1–12 (Nov 2004). <https://doi.org/10.1016/j.jcp.2004.05.012>
6. Das, S., Mullick, S.S., Suganthan, P.N.: Recent Advances in Differential Evolution – An Updated Survey. Swarm and Evolutionary Computation **27**, 1–30 (Apr 2016). <https://doi.org/10.1016/j.swevo.2016.01.004>
7. Hairer, E., Wanner, G.: Solving Ordinary Differential Equations II: Stiff and Differential-Algebraic Problems. Springer, 2nd rev. edn. (2002)
8. Hammer, J., Eitzinger, J., Hager, G., Wellein, G.: Kerncraft: A Tool for Analytic Performance Modeling of Loop Kernels. In: Tools for High Performance Computing 2016. pp. 1–22. Springer (Oct 2017). https://doi.org/10.1007/978-3-319-56702-0_1
9. Hofmann, J., Alappat, C., Hager, G., Fey, D., Wellein, G.: Bridging the Architecture Gap: Abstracting Performance-Relevant Properties of Modern Server Processors (2019), preprint

10. van der Houwen, P. J. and Sommeijer, B.P.: Parallel Iteration of High-order Runge-Kutta Methods with Stepsize Control. *J. Comput. Appl. Math.* **29**(1), 111–127 (Jan 1990). [https://doi.org/10.1016/0377-0427\(90\)90200-J](https://doi.org/10.1016/0377-0427(90)90200-J)
11. Mazzia, F., Magherini, C.: Test Set for Initial Value Problem Solvers, Release 2.4. <https://archimede.dm.uniba.it/~testset/> (Feb 2008)
12. Pfaffe, P., Grosser, T., Tillmann, M.: Efficient Hierarchical Online-Autotuning: A Case Study on Polyhedral Accelerator Mapping. In: *Proc. ACM Int. Conf. Supercomputing*. pp. 354–366. ICS '19, ACM, New York, NY, USA (2019). <https://doi.org/10.1145/3330345.3330377>
13. Rasch, A., Gorlatch, S.: ATF: A Generic Directive-Based Auto-Tuning Framework. *Concurrency Computat. Pract. Exper.* **31**(5), e4423 (Mar 2019). <https://doi.org/10.1002/cpe.4423>
14. Scherg, M., Seiferth, J., Korch, M., Rauber, T.: Performance Prediction of Explicit ODE Methods on Multi-Core Cluster Systems. In: *Proc. 2019 ACM/SPEC Int. Conf. on Performance Engineering*. pp. 139–150. ICPE '19, ACM (2019). <https://doi.org/10.1145/3297663.3310306>
15. Seiferth, J., Alappat, C., Korch, M., Rauber, T.: Applicability of the ECM Performance Model to Explicit ODE Methods on Current Multi-core Processors. In: *High Performance Computing: Proc. 33rd Int. Conf., ISC High Performance 2018*. pp. 163–183. ISC '18, Springer (Jun 2018). https://doi.org/10.1007/978-3-319-92040-5_9
16. Shudler, S., Vrabec, J., Wolf, F.: Understanding the Scalability of Molecular Simulation Using Empirical Performance Modeling. In: *Programming and Performance Visualization Tools*. pp. 125–143. Springer (2019). https://doi.org/10.1007/978-3-030-17872-7_8
17. Stengel, H., Treibig, J., Hager, G., Wellein, G.: Quantifying Performance Bottlenecks of Stencil Computations Using the Execution-Cache-Memory Model. In: *Proc. 29th ACM Int. Conf. on Supercomputing*. pp. 207–216. ICS '15, ACM (2015). <https://doi.org/10.1145/2751205.2751240>
18. Tallent, N.R., Mellor-Crummey, J.M.: Effective Performance Measurement and Analysis of Multithreaded Applications. In: *Proc. 14th ACM SIGPLAN Symp. on Principles and Practice of Parallel Programming*. pp. 229–240. PPOPP '09, ACM (Feb 2009). <https://doi.org/10.1145/1504176.1504210>
19. Tiwari, A., Hollingsworth, J.K.: Online Adaptive Code Generation and Tuning. In: *Proc. 2011 IEEE Int. Parallel Distributed Processing Symp.* pp. 879–892. IPDPS '11, IEEE (May 2011). <https://doi.org/10.1109/IPDPS.2011.86>
20. Whaley, R.C., Petitet, A., Dongarra, J.: Automated Empirical Optimizations of Software and the ATLAS Project. *Parallel Computing* **27**(1), 3–35 (Jan 2001). [https://doi.org/10.1016/S0167-8191\(00\)00087-9](https://doi.org/10.1016/S0167-8191(00)00087-9)
21. Williams, S., Waterman, A., Patterson, D.: Roofline: An Insightful Visual Performance Model for Multicore Architectures. *Communications of the ACM* **52**(4), 65–76 (Apr 2009). <https://doi.org/10.1145/1498765.1498785>